Structural insight into the mechanisms of enveloped virus tethering by tetherin

Haitao Yang[a,1], Jimin Wang[a,1], Xiaofei Jia[a], Matthew W. McNatt[b], Trinity Zang[b], Baocheng Pan[a], Wuyi Meng[a], Hong-Wei Wang[a], Paul D. Bieniasz[b], and Yong Xiong[a,2]

[a]Department of Molecular Biophysics and Biochemistry, Yale University, New Haven, CT 06520-8114; and [b]Howard Hughes Medical Institute, Aaron Diamond AIDS Research Center and Laboratory of Retrovirology, The Rockefeller University, New York, NY 10016

Edited by Stephen C. Harrison, Harvard Medical School, Boston, MA, and approved September 2, 2010 (received for review August 3, 2010)

Tetherin/BST2 is a type-II membrane protein that inhibits the release of a range of enveloped viruses, including HIV-1. Here we report three crystal structures of human tetherin, including the full-length ectodomain, a triple cysteine mutant and an ectodomain truncation. These structures show that tetherin forms a continuous alpha helix encompassing almost the entire ectodomain. Tetherin helices dimerize into parallel coiled coils via interactions throughout the C-terminal portion of the ectodomain. A comparison of the multiple structures of the tetherin dimer reveals inherent constrained flexibility at two hinges positioned at residues A88 and G109. In the crystals, two tetherin ectodomain dimers associate into a tetramer by forming an antiparallel four-helix bundle at their N termini. However, mutagenesis studies suggest that the tetrametric form of tetherin, although potentially contributing to, is not essential for its antiviral activity. Nonetheless, the structural and chemical properties of the N terminus of the ectodomain are important for optimal tethering function. This study provides detailed insight into the mechanisms by which this broad-spectrum antiviral restriction factor can function.

transmembrane | disulfide bonds | stability | budding

Tetherin (also known as BST2, CD317, and HM1.24) has recently been identified as a major host restriction factor that plays an important role in the innate immune response to viral infections. This interferon-induced antiviral protein restricts the release of HIV-1 virions (1, 2) and many other enveloped viruses (3–5) from infected cells. Tetherin is active against members of at least four virus families: retroviruses, filoviruses, arenaviruses, and herpesviruses (6) and is thus a key component of the innate immune system. To evade this component of the host antiviral response, HIV-1 expresses viral protein U (Vpu), which down-regulates tetherin from the plasma membrane (1, 2, 7–12). Similarly, proteins encoded by other enveloped viruses have evolved to antagonize tetherin, such as simian immunodeficiency virus (SIV) Nef, HIV-2 and SIV Env, Ebola glycoprotein, and the K5 protein of Kaposi's sarcoma-associated herpesvirus (5, 13–16).

Tetherin is a transmembrane protein with a unique topology. It has a short cytoplasmic tail at the N terminus followed by a transmembrane (TM) region, a ~110 amino acid ectodomain (ED), and a C-terminal glycosyl phosphatidylinositol (GPI) anchor. Recent work shows that tetherin is incorporated into HIV-1 virions and directly bridges viral and infected cell membranes (17–20) by inserting its membrane anchors into virions as a parallel homodimer (17). Three cysteines (C53/C63/C91) in the ED may stabilize dimerization by forming disulfide bonds (17, 21). The tethering mechanisms of tetherin remain largely unknown, despite several hypotheses derived from functional studies (17, 18, 20) and a crystal structure of an ED fragment (22).

We have determined crystal structures of three tetherin ED constructs in four crystal forms at resolutions of 2.3 Å–3.2 Å. These include a full-length tetherin ED, (residues 47–161, two crystal forms), a triple mutant of tetherin ED with all three cysteines mutated to alanines (tetherin ED-3A, C53A/C63A/C91A), and a C-terminal truncation of tetherin ED-3A fused with maltose binding protein (MBP-tetherin ED-3A-N, residues 52–139). These structures, together with biochemical and functional analyses, establish a framework for understanding the structural basis of tetherin's antiviral function.

Results

Overall Structures. To describe the tetherin ED structure, we divide it into the head (residues 50–84), the neck (85–90), the body (91–150), and the tail (151–158) (Fig. 1). The entire ectodomain is observed in the current structures with the tip of the head positioned three amino acids away from the transmembrane region and the end of the tail positioned two amino acids away from the GPI anchor. The tetherin ED forms a 165-Å-long continuous α-helix spanning almost the entire ED (including the head, neck, and body) (Fig. 1*B*). The neck and the body dimerize to form a left-handed parallel coiled coil, whereas the head adopts a more open conformation, and the tail has multiple flexible conformations in different crystals (Fig. 1*B*). Surprisingly, all tetherin ED dimers further associate head to head, forming a 275-Å-long tetramer of an antiparallel 4-helix bundle between flanking coiled coils (Fig. 1*A*). The neck region is defined for residues from at the boundary of the 4-helix bundle to around a major flexible region in the coiled-coil dimer (discussed below). N65 and N92, the two glycosylation sites, are solvent exposed and accessible for modification (Fig. 1*B*).

The MBP-fused tetherin ED forms essentially the same structure, but has a bending of ~40° in the body region due to packing interactions with MBP (Fig. 1*C*). In this construct, the C-terminal helix of MBP is fused to the N terminus of the tetherin ED with a short linker, simulating the possible orientation of the transmembrane helix connected to the tetherin ED. The MBP helix is observed at various angles (50°–150°) relative to the tetherin ED (Fig. 1*D*), implying a topological flexibility in the relationship between the tetherin ED and the transmembrane helix.

A Stable Tetherin Dimer with Inherent Flexibility. The tetherin ED neck and body adopt the classic coiled-coil conformation with a repeat of seven amino acids (heptad) denoted "a" to "g," where hydrophobic residues in the a and d positions constitute the structural core, and charged residues in the e and g positions form stabilizing salt bridges. There are 17 helical turns in the parallel

Author contributions: H.Y., P.D.B., and Y.X. designed research; H.Y., X.J., M.W.M., T.Z., B.P., H.-W.W., and Y.X. performed research; H.-W.W. and P.D.B. contributed new reagents/analytic tools; H.Y., J.W., W.M., P.D.B., and Y.X. analyzed data; and H.Y. and Y.X. wrote the paper.

The authors declare no conflict of interest.

This article is a PNAS Direct Submission.

Data deposition: The atomic coordinates and structure factors have been deposited in the Protein Data Bank, www.pdb.org (PDB ID codes 3MQ7, 3MQC, 3MQB, and 3MQ9).

[1]H.Y. and J.W. contributed equally to this work.

[2]To whom correspondence should be addressed. E-mail: yong.xiong@yale.edu.

This article contains supporting information online at www.pnas.org/lookup/suppl/doi:10.1073/pnas.1011485107/-/DCSupplemental.

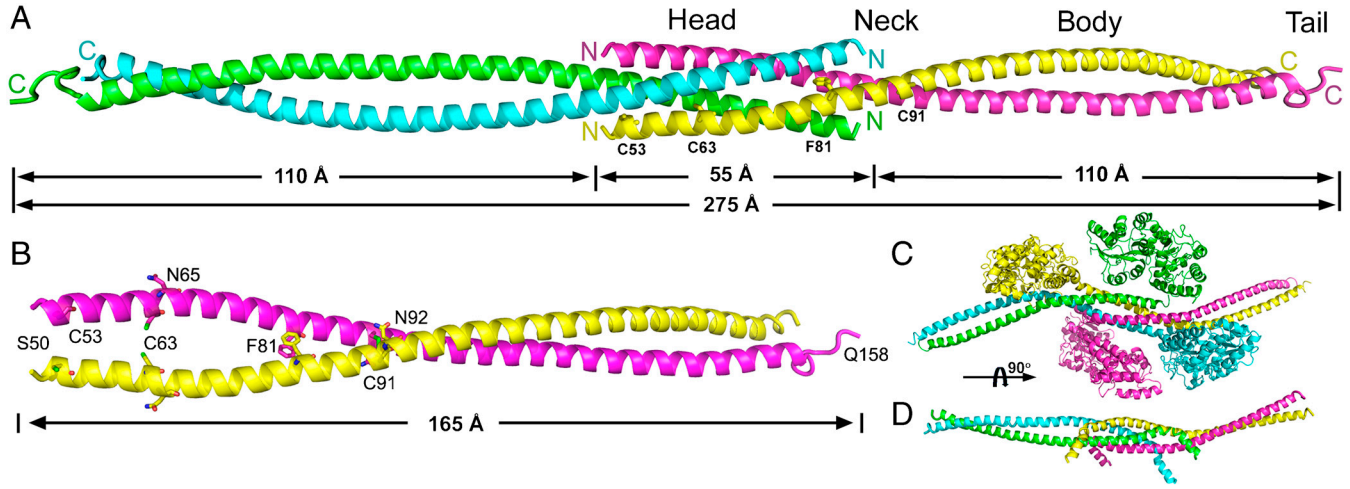

Fig. 1. The crystal structures of the tetherin ectodomain (tetherin ED). (*A*) Ribbon representation of the tetherin ED tetramer. (*B*) The tetherin ED dimer with selected residues (ball and sticks) marked. (*C*) Ribbon representation of the MBP-fused tetherin ED structure. (*D*) The C-terminal helices (MBP) in the MBP-tetherin ED-3A-N structure suggest potential orientations of the tetherin transmembrane helix.

coiled coil, burying 2,976 Å^2 of hydrophobic surface area in a stable dimer (Fig. 2). Packing defects (holes) exist in two positions in the core of the coiled coil, at residues A88 and G109 (Fig. 2*A*). The presence of G109 ("stutter") in a "d" position also shifts the positions of the hydrophobic core residues (Fig. S1).

The packing holes at positions A88 and G109 result in two hinge regions that allow modest bending of the coiled-coil dimer (Fig. 2 *A–D*). The many independent tetherin ED dimers, observed in multiple crystals, allow for an assessment of the inherent flexibility at the two hinge positions. Superposition of 10 independent tetherin ED dimers shows that a major bending occurs at hinge 1 (A88) with various degrees of bending up to ~25° (Fig. 2*B*). Hinge 2 at G109 endows the tetherin ED an additional degree of flexibility, which facilitates bending up to ~18° (Fig. 2*D*). A recently reported structure of the tetherin ED body falls into our observed range of flexibility (22). Because of geometrical constrainst, bending at any given position in a coiled-coil helix normally occurs in the direction facing the grooves of the superhelical structure. Interestingly, the locations of the two hinge regions in the tetherin ED coiled coil create two perpendicular bending directions that produce a full range of motions (Fig. 2 *B–D*). This inherent but constrained flexibility may enhance the antiviral tethering ability of tetherin.

Disulfide Bonds Are Required for a Stable Dimeric Tetherin Head. The head domain of tetherin ED adopts an open conformation in an otherwise nearly continuous coiled coil stemming from the neck and body (Figs. 1*B* and 2*E*). An inspection of the shape and surface charge distribution reveals that the head domain cannot dimerize stably as a normal coiled coil. In particular, close packing of the two α-helices cannot occur because of mismatched residue sizes along the superhelical path. For example, residues in the coiled-coil core form knob-knob (e.g., F81-F81) and hole-hole (e.g., G56-G56) "interactions," thus preventing close packing (Fig. 2*E*). Additionally, an uneven distribution of charged residues in the e and g positions leads to an unbalanced positive charge at the tip of the head but a net negative charge near the neck (Fig. 2*F*), further inhibiting lateral interaction of the two head regions within a dimer. The open form of the tetherin head is presumably flexible and vulnerable for hydrolysis in solution. During purification of the tetherin ED-3A construct (Cys mutant), where no disulfide bonds can be formed to stabilize the head, we observed a much higher degree of degradation over time compared with the WT tetherin ED.

Disulfide bonds formed by pairs of residues C53 and C63 may stabilize the tetherin ED head in a dimeric conformation. All three cysteines in the tetherin ED (C53, C63, and C91) showed the ability to form disulfide bonds in functional studies (17, 21). In both WT tetherin ED structures, the pair of C91 residues in the coiled-coil body forms a disulfide bond (Fig. 1*B* and Fig. S2*F*). Unexpectedly, in our structures, no disulfide bonds are formed by residues C53 and C63. The S-S distances are 8.2 Å and 6.9 Å for the C53 and C63 pairs, respectively (Fig. S2 *A* and *D*). The crys-

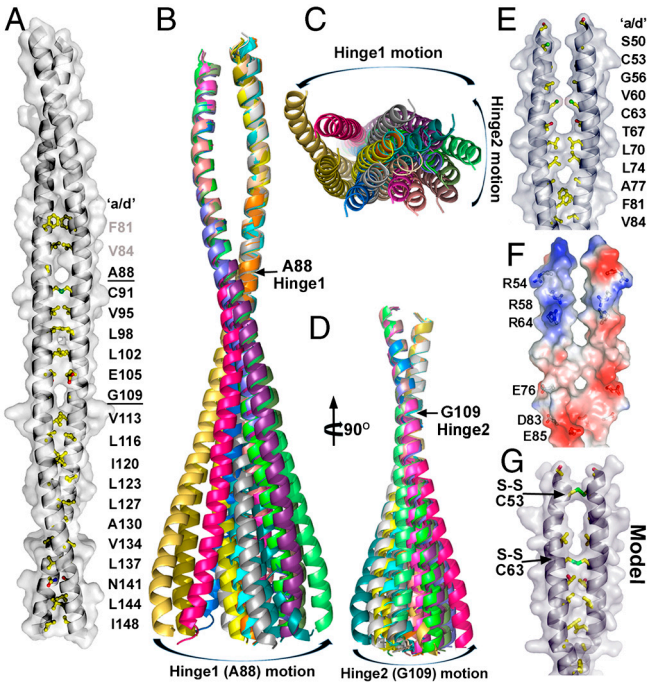

Fig. 2. (*A*) Interactions in the tetherin ED dimer, shown as ribbons under the molecular surface. Hydrophobic core residues ("a/d") are shown as ball and stick. Sulfur atoms and S-S bonds are shown in green. (*B*) Superposition of 10 independent tetherin ED dimer heads shows flexibility around A88. (*C*) The range of motions as seen from the bottom view from the orientation in *B*. (*D*) Superposition of residues A88–G109 in the 10 independent tetherin ED dimers shows flexibility around G109. (*E* and *F*) The tetherin ED head does not form a stable dimer and shows size/shape (*E*) and charge (*F*) complementarity between upper and lower halves. (*G*) Model of C53/C63 disulfide-linked head dimer.

tallization condition of the ED requires a mixture of reducing agent [0.2–0.5 mM Tris(2-carboxyethyl)phosphine] and oxidizing agent (3%–6% DMSO). This redox environment presumably resulted in the formation of disulfide bonds between the C91 pairs, but not between the C53 pairs or the C63 pairs in the crystal.

To understand the property of the disulfide-linked head dimer, we carried out molecular dynamics modeling of the tetherin ED structure with C53/C63 disulfide bonds, using simulated annealing and energy minimization implemented in the crystallographic program CNS (23, 24). As expected, the C53/C63 disulfide bonds can maintain the tetherin ED head in a more closely packed dimeric configuration with slight reorientation of the bulky side chains from the core residues; however, a large packing void remains at the site of the smaller core residues (Fig. 2*G*) at the tip of the head. This configuration presumably endows the tetherin ED additional degree of flexibility and contributes to its activity. The result reinforces that the C53/C63 disulfide bonds are required to maintain the head dimer, and they may be relatively unstable because of the energetic cost from bringing together the tetherin heads with unmatched size and charge. This may explain our observation of the C91 disulfide bond but not those from C53/C63 in the crystals. This has been corroborated by in vitro biochemical data showing that the elimination of the third disulfide bond (C91A mutation) dramatically reduces disulfide-linked dimerization even with C53 and C63 intact (22). Functionally, these disulfide bonds are shown to be important, but not essential for the antiviral activity of tetherin (17, 21, 25). The disulfide-linked tetherin ED head may be evolved as a balance of stability and flexibility for optimal viral tethering.

Four-Helix Bundle Interaction at the Tetherin Head. In the absence of C53/C63 disulfide bonds, the opening of the tetherin ED dimer at its head enables the unexpected tetramerization of two coiled coils through a 4-helix bundle of 10 helical turns (Fig. 3 *A* and *B*). Formation of the 4-helix bundle results in a large, mostly hydrophobic buried surface area of 2,840 Å^2 per parallel dimer through an intricate set of knob-into-hole packing interactions in its 4-helix bundle core (Figs. S2 and S3). Bulkier residues form an interaction diagonally across two parallel helices, and adjacent, smaller side chain pairs from the inverted parallel chains pack onto the bulky diagonal residues. For example, in the second layer of the 4-helix bundle, four glycines surround the aromatic side chains of two phenylalanines (Fig. 3*B*).

The observed tetherin ED tetramer is not a result of crystal packing, even though it likely does not play a major role in the antiviral function of tetherin (see data and discussion below). The tetramer is observed eight times in independent crystal packing environments, including within a MBP fusion construct. We further used size-exclusion chromatography and multiangle laser light scattering to verify that tetherin ED exists in solution as a mixture of dimers and tetramers, albeit with the disulfide-linked dimers as the major form (Fig. S4). We also examined the purified tetherin ED under a transmission electron microscope and observed filaments with a length of 25 ± 7 nm (Fig. S2*G*), in good agreement with the 275-Å tetramer in the crystals.

Antiviral Activity Assay of Tetherin Head Mutants. To investigate potential functional importance of the tetherin head, several mutations were introduced to this region of tetherin. Infectious virion release was evaluated after transfection of 293T cells with HIV-1(WT) or HIV-1(ΔVpu) proviral plasmids, along with varying amounts of plasmids expressing WT or one of the mutant tetherin-HA proteins. The cellular localization of the mutants was examined by immunofluorescence microscopy (Fig. 3*E*).

Two deletion mutations targeting the tetherin head domain, namely Δ60–85 and Δ70–85, reduced but did not eliminate tetherin's antiviral activity (Fig. 3 *D*–*F*). These deletions remove the bulk of the head domain and would very likely abolish tetramer formation. The considerable residual antiviral activity exhibited by these mutants indicates that the dimeric form of tetherin is functional, consistent with the fact that the artificial tetherin

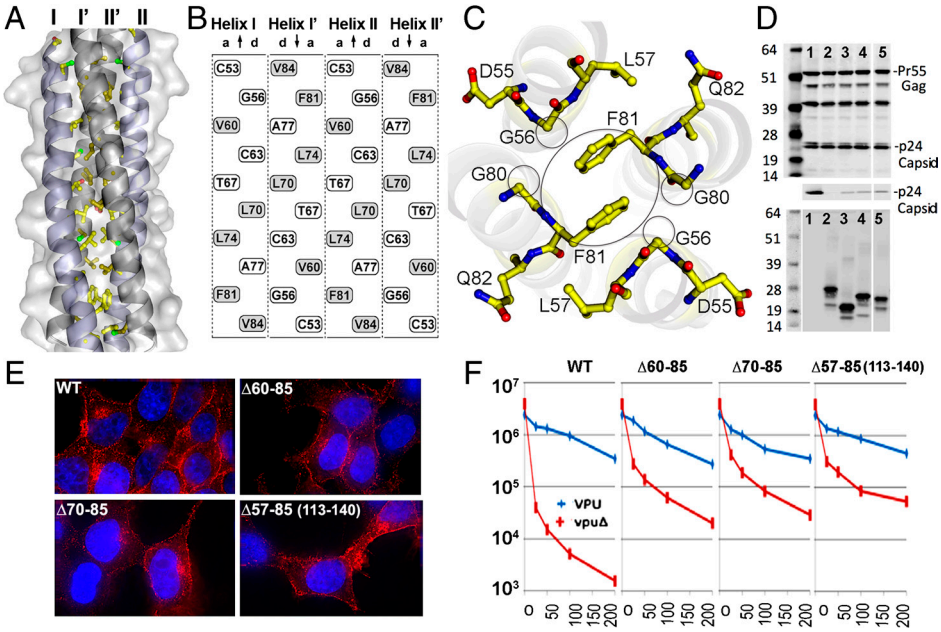

Fig. 3. (*A*) Interactions in the tetherin ED head tetramer, shown as ribbons under the molecular surface. Hydrophobic core residues (a/d) are shown as ball and stick. I' and II' denote the inverse chains of the parallel helices I and II, respectively. (*B*) An "opened out and flattened" representation of the packing layers in the 4-helix bundle of tetherin ED showing the amino acids present in the a and d positions of the core. The larger residues are in gray. (*C*) Packing interactions in the F81 layer of the tetherin ED 4-helix bundle. (*D*) Western blot analysis [anti-Gag antibody (*Upper*) and anti-HA (*Lower*)] of cell lysates and corresponding virion pellets (*Middle*) following transfection of proviral plasmids and plasmids expressing WT and mutant tetherins (lane numbers 1–5 represent mock, WT, and different tetherin mutants corresponding to panels in *F*). (*E*) Immunofluorescent microscopic images of the cellular localization of the tetherin mutants. (*F*) Infectious virion release was evaluated after transfection of 293T cells with HIV-1(WT) or HIV-1(ΔVpu) proviral plasmids, along with varying amounts of WT and tetherin mutant plasmids as indicated.

constructed with fragments of unrelated proteins can restrict the release of HIV-1 virions (17). Nonetheless, the antiviral activity of the deletion mutants was reduced by more than 10-fold compared with WT tetherin.

To test whether the reduced activity of the tetherin head deletion mutants was simply due to a reduced length of the extracellular domain, we generated the chimeric mutant Δ57–85 (113–140) by replacing a deleted head region (residues 57–85) with a stable dimeric fragment from the body domain (residues 113–140). This manipulation retains the authentic length of the tetherin ED and two of the three disulfide bonds. However, it results in a molecule where the properties of the head domain are obviously altered with a high likelihood to form a stable, tightly packed dimer. The resulting mutant has a similar antiviral activity to the head domain deletion mutants (Fig. 3*F*). These data support the notion that the properties of the tetherin head, particularly the deviation from a canonical tightly packed coiled coil, can significantly enhance the antiviral activity of tetherin.

Notably, the tetherin ED dimer has an uneven distribution of charged residues, resulting in a bias of positively charged residues on the surface of the tetherin dimer near the membrane anchors at both ends of tetherin ED (Fig. 4*A*), and accumulation of negatively charged residues at close to the center of the dimeric tetherin ED. This biased charge distribution is evident in the head domain, and we examined the functional importance of this biased charge distribution therein. Notably, reversing charges in clusters of positive and negative residues, such as R54D/R58D/R64D and E76R/D83R/E85R, resulted in a ∼10-fold loss of antiviral activity (Fig. 4*B*). When these mutations were combined resulting in a reversal of the charge bias in the head domain (R54D/R58D/R64D/E76R/D83R/E85R), a ∼100-fold loss in antiviral activity was observed. These results suggest that the clusters of charged residues, particularly those in the tetherin head domain, contribute to tetherin function, perhaps through opposing interactions with the negatively charged phospholipids of cellular and virion membranes or by maintaining specific structural properties of the tetherin head.

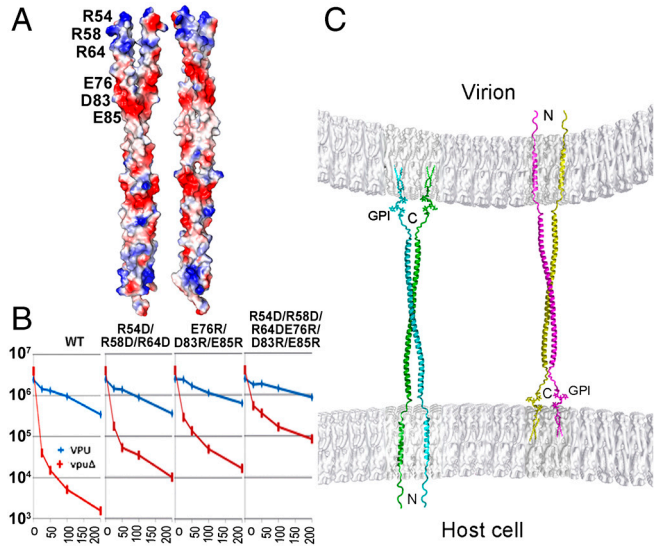

Fig. 4. (*A*) The electrostatic surface potential of tetherin ED dimers and tetramers, respectively, in two perpendicular views. Note the positive charge (blue) toward both ends of the dimer and a negative charge (red) toward the center of the dimer. (*B*) Analysis of antiviral activity of tetherin mutants that change the surface charge distribution in the head. (*C*) Dimeric tethering model drawn to the correct relative scale. The lipid bilayers are constructed using coordinates of phospholipids.

Discussion

The interferon-induced antiviral protein tetherin functions by directly tethering enveloped virus particles that bud through the plasma membrane (17). The work reported herein provides detailed insight of the mechanisms by which tetherin functions. Indeed consistent with its function as a direct tether, the structure of the entire ectodomain of tetherin is a single, long α-helix that forms a parallel coiled coil with a second molecule of tetherin. These parallel dimers could bridge viral and host cell membranes by incorporating one end (either N or C) into the viral membrane, whereas the opposite end remains embedded in the cellular membrane (Fig. 4*C*). In this configuration, all three cysteines could form disulfide bonds, stabilizing the head domain to maintain virtually the entire ectodomain in an extended coiled-coil-like structure. Additionally, the multiple structures reported herein reveal the inherent, but constrained, flexibility in the tetherin ED. Thus, maintaining the maximal spatial separation of the membrane anchors while endowing flexibility might be a strategy to maximize the likelihood of only one pair of anchors being incorporated into the virion envelope, resulting in viral tethering. Moreover, the charge distribution in the tetherin ED dimer (Fig. 4*A*) shows a positive charge bias toward both termini and negative charge toward the center. This gives rise to the prediction that only the ends of the tetherin ED dimer are anchored close to the negatively charged membrane. Interestingly, the biased charge distribution, particularly the repulsion of the membrane surface by the central portion the tetherin dimer, could potentially introduce tension and favor the localization of tetherin to "inwardly" curving membranes; such as those at the neck of a budding virion, thus allowing the negatively charged central region of the tetherin ED to be spatially separated from the membrane.

We observed the unexpected formation of tetherin tetramers in our crystals. The tetrameric tetherin's biological function is not clear and a number of lines of evidence indicate that it may not play a critical role in its antiviral function. First, all three cysteines were shown to form disulfide bonds in mammalian cells, and the formation of disulfide bonds at C53/C63 is topologically incompatible with the assembly of the tetramer; i.e., covalently linked N-termini of parallel tetherin ED dimers would prevent tetramer formation. It is formally possible that disulfide bonds formed initially could be broken by thiol-disulfide exchange enzymes, such as protein disulfide isomerase, which reduces several disulfide bonds in HIV-1 gp120 during the fusogenic activation of viral entry (26). However, there is as yet no evidence for this to occur in tetherin. Second, our deletion mutations, which disrupt the formation of the tetramer, retain substantial function, confirming that the dimeric form of tetherin is sufficient for tethering. Third, although we verified the existence of a stable tetramer in solution in vitro, there is precedent for nonphysiological association of recombinant coiled-coil proteins (27). Nevertheless, we cannot exclude the possibility of a tethering mode in which a tetherin tetramer with eight membrane anchors that partition between virion and host membranes serves as a tether to retain virions close to the host cell membrane (Fig. S5). Alternatively, a terameric form of tetherin may play other potential roles, such as providing molecular stability prior to C53/C63 disulfide bonds formation. It has been observed that a high-mannose form of tetherin, presumably those molecules not yet exited the endoplasmic reticulum, does not form disulfide-linked dimers (21). Overall these results establish a mechanistic framework for understanding the function of this broad-spectrum antiviral membrane tether and point to potential previously undescribed directions in further elucidating the details of how viruses are tethered and how they evade the tetherin function.

Methods

For mammalian expression, tetherin ED was expressed in 293T cells and purified by nickel affinity column. For bacterial expression, tetherin ED, tetherin ED-3A, and MBP-tetherin ED-3A-N were expressed in *Escherichia coli* and purified using affinity, ion-exchange, and size-exclusion chromatography. Crystals were grown under oil, and diffraction data were collected at the Advanced Photon Source beamline 24-ID and the National Synchrotron Light Source beamlines X25 and X29. The crystals showed strong anisotropic diffraction (Fig. S6). The structure of tetherin ED-3A was determined by the Se-multiple wavelength anomalous dispersion method. The two tetherin ED-WT structures were solved by molecular replacement using the tetherin ED-3A structure as a search model. The structure of MBP-tetherin ED-3A-N was solved by molecular replacement using a ligand-free MBP structure (1PEB) as a search model. Diffraction data and refinement statistics are summarized in Table S1. C53/C63 disulfide-linked dimer was carried out using CNS (23, 24). Negative stain electron microscopy data were collected using a FEI T12 microscope. Multiangle laser light-scattering experiments were performed on a DAWN EOS spectrometer coupled to an OPTILAB DSP interferometric refractometer (Wyatt Technologies). Immunofluorescent microscopy was done using a Deltavision suite (Applied Precision) as described previously (1). For antiviral activity assay, infectious virion release was evaluated after transfection of 293T cells with HIV-1(WT) or HIV-1(delVpu) proviral plasmids, along with varying amounts of tetherin plasmids expressing WT or one of the mutant tetherin proteins. Detailed methods are described in *SI Text*.

ACKNOWLEDGMENTS. We thank Walther Mothes, Leslie Wolfe, William Eliason, Lynne Regan, Karin Reinisch, and Yorgo Modis for assistance and encouragement. We also thank the staff at the Advanced Photon Source beamline 24-ID and the staff at National Synchrotron Light Source beamlines X25 and X29A. This work was supported by National Institutes of Health Grants AI078831 (to Y.X.) and AI050111 (to P.D.B.).

1. Neil SJ, Zang T, Bieniasz PD (2008) Tetherin inhibits retrovirus release and is antagonized by HIV-1 Vpu. *Nature* 451:425–430.
2. Van Damme N, et al. (2008) The interferon-induced protein BST-2 restricts HIV-1 release and is downregulated from the cell surface by the viral Vpu protein. *Cell Host Microbe* 3:245–252.
3. Jouvenet N, et al. (2009) Broad-spectrum inhibition of retroviral and filoviral particle release by tetherin. *J Virol* 83:1837–1844.
4. Sakuma T, Noda T, Urata S, Kawaoka Y, Yasuda J (2009) Inhibition of Lassa and Marburg virus production by tetherin. *J Virol* 83:2382–2385.
5. Kaletsky RL, Francica JR, Agrawal-Gamse C, Bates P (2009) Tetherin-mediated restriction of filovirus budding is antagonized by the Ebola glycoprotein. *Proc Natl Acad Sci USA* 106:2886–2891.
6. Tokarev A, Skasko M, Fitzpatrick K, Guatelli J (2009) Antiviral activity of the interferon-induced cellular protein BST-2/tetherin. *AIDS Res Hum Retroviruses* 25:1197–1210.
7. Dube M, et al. (2010) Antagonism of tetherin restriction of HIV-1 release by Vpu involves binding and sequestration of the restriction factor in a perinuclear compartment. *PLoS Pathog* 6:e1000856.
8. Douglas JL, et al. (2009) Vpu directs the degradation of the human immunodeficiency virus restriction factor BST-2/Tetherin via a βTrCP-dependent mechanism. *J Virol* 83:7931–7947.
9. Mangeat B, et al. (2009) HIV-1 Vpu neutralizes the antiviral factor Tetherin/BST-2 by binding it and directing its beta-TrCP2-dependent degradation. *PLoS Pathog* 5: e1000574.
10. Iwabu Y, et al. (2009) HIV-1 accessory protein Vpu internalizes cell-surface BST-2/tetherin through transmembrane interactions leading to lysosomes. *J Biol Chem* 284:35060–35072.
11. Mitchell RS, et al. (2009) Vpu antagonizes BST-2-mediated restriction of HIV-1 release via beta-TrCP and endo-lysosomal trafficking. *PLoS Pathog* 5:e1000450.
12. Goffinet C, et al. (2009) HIV-1 antagonism of CD317 is species specific and involves Vpu-mediated proteasomal degradation of the restriction factor. *Cell Host Microbe* 5:285–297.
13. Jia B, et al. (2009) Species-specific activity of SIV Nef and HIV-1 Vpu in overcoming restriction by tetherin/BST2. *PLoS Pathog* 5:e1000429.
14. Le Tortorec A, Neil SJ (2009) Antagonism to and intracellular sequestration of human tetherin by the human immunodeficiency virus type 2 envelope glycoprotein. *J Virol* 83:11966–11978.
15. Mansouri M, et al. (2009) Molecular mechanism of BST2/tetherin downregulation by K5/MIR2 of Kaposi's sarcoma-associated herpesvirus. *J Virol* 83:9672–9681.
16. Zhang F, et al. (2009) Nef proteins from simian immunodeficiency viruses are tetherin antagonists. *Cell Host Microbe* 6:54–67.
17. Perez-Caballero D, et al. (2009) Tetherin inhibits HIV-1 release by directly tethering virions to cells. *Cell* 139:499–511.
18. Fitzpatrick K, et al. (2010) Direct restriction of virus release and incorporation of the interferon-induced protein BST-2 into HIV-1 particles. *PLoS Pathog* 6:e1000701.
19. Hammonds J, Wang JJ, Yi H, Spearman P (2010) Immunoelectron microscopic evidence for Tetherin/BST2 as the physical bridge between HIV-1 virions and the plasma membrane. *PLoS Pathog* 6:e1000749.
20. Habermann A, et al. (2010) CD317/tetherin is enriched in the HIV-1 envelope and downregulated from the plasma membrane upon virus infection. *J Virol* 84:4646–4658.
21. Andrew AJ, Miyagi E, Kao S, Strebel K (2009) The formation of cysteine-linked dimers of BST-2/tetherin is important for inhibition of HIV-1 virus release but not for sensitivity to Vpu. *Retrovirology* 6:80.
22. Hinz A, et al. (2010) Structural basis of HIV-1 tethering to membranes by the BST-2/tetherin ectodomain. *Cell Host Microbe*, 7 pp:314–323.
23. Brunger AT (2007) Version 1.2 of the crystallography and NMR system. *Nat Protoc* 2:2728–2733.
24. Brunger AT, et al. (1998) Crystallography & NMR system: A new software suite for macromolecular structure determination. *Acta Crystallogr D* 54:905–921.
25. Sakuma T, Sakurai A, Yasuda J (2009) Dimerization of tetherin is not essential for its antiviral activity against Lassa and Marburg viruses. *PLoS One* 4:e6934.
26. Ryser HJ, Fluckiger R (2005) Progress in targeting HIV-1 entry. *Drug Discov Today* 10:1085–1094.
27. Freedman SJ, Song HK, Xu Y, Sun ZY, Eck MJ (2003) Homotetrameric structure of the SNAP-23 N-terminal coiled-coil domain. *J Biol Chem* 278:13462–13467.